Superresolving Phase Measurement with Short-Wavelength NOON States by Quantum Frequency Up-Conversion

Zhi-Yuan Zhou,[1,2,*] Shi-Long Liu,[1,2] Shi-Kai Liu,[1,2] Yin-Hai Li,[3] Dong-Sheng Ding,[1,2] Guang-Can Guo,[1,2] and Bao-Sen Shi[1,2,†]

[1]*CAS Key Laboratory of Quantum Information, USTC, Hefei, Anhui 230026, China*
[2]*Synergetic Innovation Center of Quantum Information & Quantum Physics, University of Science and Technology of China, Hefei, Anhui 230026, China*
[3]*Department of Optics and Optical Engineering, University of Science and Technology of China, Hefei, Anhui 230026, China*

(Received 24 January 2017; revised manuscript received 23 April 2017; published 26 June 2017; corrected 27 October 2020)

Precise measurements are the key to advances in all fields of science. Quantum entanglement shows higher sensitivity than that which is achievable by classical methods. Most physical quantities including position, displacement, distance, angle, and optical path length can be obtained by optical phase measurements. Reducing the photon wavelength of the interferometry can further enhance the optical-path-length sensitivity and imaging resolution. By quantum frequency up-conversion, we realize a short-wavelength two-photon number entangled state. Nearly perfect Hong-Ou-Mandel interference is achieved after both 1547-nm photons are up-converted to 525 nm. Optical phase measurement of the two-photon entanglement state yields a visibility greater than the threshold to surpass the standard quantum limit. A spectra change of the photon pair after being up-converted is observed and well explained. These results offer alternative ways for high-precision quantum metrology using a short-wavelength quantum entanglement number state and offer a potential all-optical spectra engineering technique for the photon pair source.

DOI: 10.1103/PhysRevApplied.7.064025

I. INTRODUCTION

Important in nearly all fields of science, precision measurements have been the long-pursued goal in physical science and a window to discoveries. Quantum metrology takes advantage of quantum entanglements to advance precision measurements beyond that achievable with classical methods [1]. A particularly useful class of states are maximally path-entangled multiphoton states (NOON states) $|N::0\rangle = 1/\sqrt{2}(|N0\rangle_{AB} + |0N\rangle_{AB})$, which contain N indistinguishable particles in an equal superposition with all particles being in one of the paths A and B. By measuring the phase with an N-particle NOON state, the precision of the measurement is $\Delta\phi = 1/N$—the Heisenberg limit; for measurements with N uncorrelated photons, the precision of the measurement is $\Delta\phi = 1/\sqrt{N}$—the standard quantum limit (SQL). This super-sensitivity of the phase measurement has many important applications including imaging, microscopy, gravity-wave detection, measurement of material properties, and chemical and biological sensing [2–4].

The $N\phi$ dependence of the N-particle NOON state is a manifestation of the N-photon de Broglie wavelength λ/N [5]. Referred to as phase superresolution, this dependence is responsible for an interference oscillation N times faster than that of a single photon. The observation of the reduced de Broglie wavelength has been reported for two to six photons [6–15]. Observing the reduced de Broglie wavelength does not guarantee beating SQL [11,13]. The maximum photon number surpassing SQL reported is four [13]; most of the previous experiments that beat SQL are limited to two photons. To reduce the effective de Broglie wavelength, another effective way is to reduce the fundamental wavelength of the photon. Short wavelength photons can further enhance the sensitivity in optical-path-length measurement and reduce diffraction effects in imaging. Quantum frequency conversion (QFC) is a promising technique to change the frequency of a photon while retaining its quantum properties [16]. Much progress has been achieved for QFC covering aspects such as performing complete Bell-state measurement for the polarization state in quantum teleportation [17], up-conversion of the telecom-band time-bin entanglement state [18], single-photon generation from quantum dot [19], squeezing vacuum states [20], orbital angular momentum single-photon and entangled states [21,22], fabrication of up-conversion single-photon detectors [23], and the development of frequency-domain Hong-Ou-Mandel (HOM) interference [24]. To date, the shortest wavelength entanglement generated is 390-nm polarization entanglement, which is based on biexciton resonant

*Corresponding author.
zyzhouphy@ustc.edu.cn
†Corresponding author.
drshi@ustc.edu.cn

hyperparametric scattering in a semiconductor [25]. By using the QFC technique, the achieved wavelength of the entanglement state can be even shorter than 390 nm. Though HOM interference has been realized after nondegenerate photon pairs generated by spontaneous four-wave mixing in dispersion-shifted fiber are up-converted to erase their frequency distinguishability, the interference measurements of the NOON state are not verified [26]. In trapped-iron systems, HOM interference has been realized between two short-wavelength single photons generated from two independently trapped barium ions or calcium ions, but the interference measurements of the NOON state are also not verified [27].

In this work, using the QFC technique, both photons in the pair at 1547 nm are up-converted to 525 nm. The indistinguishability of the photon pair after up-conversion is preserved and demonstrated using nearly perfect HOM interference between the two 525-nm photons. Phase measurements of the 525-nm two-photon NOON state generated yield a visibility greater than the threshold to surpass the SQL. Such 525-nm two-photon NOON states are equivalent to a 1547-nm six-photon NOON states. In addition, direct up-conversion of the 1547-nm two-photon Fock state to 525 nm is also demonstrated. A spectra change of the photon pair after being up-converted is observed and well explained. These results suggest alternative techniques for high-precision measurements based on short-wavelength NOON states of a high photon number and provide a potential all-optical spectra engineering technique for the photon pair source.

II. THEORETICAL DESCRIPTION OF QFC

QFC can be accomplished using sum frequency generation (SFG), in which the annihilation of a strong pump photon (ω_p) and a weak signal photon (ω_1) creates a SFG photon with frequency ($\omega_2 = \omega_1 + \omega_p$). The effective Hamilton operator for this process is [16]

$$\hat{H}_{\text{eff}} = i\hbar\xi(\hat{a}_1\hat{a}_2^{\dagger} - \hat{a}_1^{\dagger}\hat{a}_2), \tag{1}$$

where $\hat{a}_1$ and $\hat{a}_2^{\dagger}$ represent, respectively, the annihilation and creation operators of the signal and SFG photons; ξ is a constant, which is proportional to the product of the pump amplitude E_p and the second-order susceptibility $\chi^{(2)}$. The evolution of $\hat{a}_j$ obtained in the Heisenberg's picture is given as

$$\hat{a}_1(t) = \hat{a}_1(0)\cos(\xi t) - \hat{a}_2(0)\sin(\xi t), \tag{2}$$

$$\hat{a}_2(t) = \hat{a}_2(0)\cos(\xi t) + \hat{a}_1(0)\sin(\xi t). \tag{3}$$

When $\xi t_f = \pi/2$, the input signal field is completely converted to the output SFG field $\hat{a}_2(t_f) = \hat{a}_1(0)$. As ξ strongly depends on the pump amplitude, the key point for reaching maximum conversion efficiency is to increase the pump power. In this article, the conversion efficiency is increased using a ring cavity to enhance the pump power.

III. QFC FOR THE TWO-PHOTON FOCK STATE

We first up-convert the two-photon Fock state $|02\rangle_{1547\text{ nm}}$ generated from the HOM interference of the 1547-nm telecom-band photon pair. In the experimental setups (Fig. 1), the 1547-nm photon source [Fig. 1(a)] used is generated from a 2-cm length type-II periodically poled potassium titanyl phosphate (PPKTP) crystal in a Sagnac-loop interferometer, which is pumped using a 90-mW 773.5-nm laser. The source is of high brightness and compact and high entanglement quality. The detailed

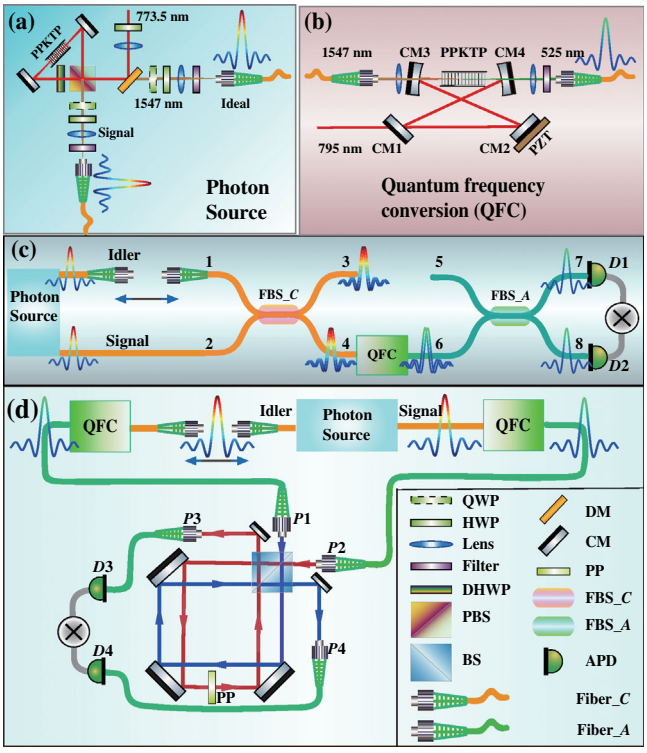

FIG. 1. Experimental setup for each experiment. (a) Simplified diagram of the single-photon source used in experiments. (b) Key module used for frequency up-conversion, in which a 1547-nm photon is focused into the center of a 2-cm type-I PPKTP crystal inside a ring cavity of single resonance at 795 nm, and is up-converted to a 525-nm photon that is collected by a single-mode fiber for detection or further processing. (c) Diagram for QFC of two-photon Fock state. (d) Setup for up-conversion of both 1547-nm photons to generate the 525-nm two-photon NOON state and perform phase measurements of this state in a self-stable tilted Sagnac interferometer. M, mirrors; QWP (HWP), quarter- (half-) wave plate; DHWP, double half-wave plate at 773.5 and 1547 nm; FC, fiber coupler; PP, phase plate; BS, beam splitter; CM, cavity mirror; DM, dichromatic mirror; PBS, polarized beam splitter; APD, avalanched single-photon detector.

performance of the source can be found in Ref. [28], the difference from Ref. [28] is that the crystal length is increased from 1 to 2 cm, which has a narrower photon-emission bandwidth of 1.28 nm. In these experiments, the pump laser of the source is from a self-building doubling laser, which can provide more than 300-mW power of a 773.5-nm laser beam [29]. The source emits degenerate photon pairs at 1547 nm. By rotating the wave plate at the input port of the Sagnac loop, the pump power circulates in the clockwise direction, therefore the polarization orthogonal photon pair is generated, the pair is separated by PBS and collected to single mode fibers (SMF). The polarization of the photon inside the SMFs is controlled by two groups of wave plates at the output ports behind the PBS.

The dependence of the internal quantum efficiency on circulation power for the QFC module is characterized by using a coherent continuous narrow-bandwidth laser source as the signal. The results are shown in Fig. 2. The maximum quantum efficiency measured is 0.37 for a pump power of 660 mW. In the sequent experiments, the internal conversion efficiencies for both cavities are maintained at around 0.16 because the total output power of our Ti: sapphire laser is limited to 1.5 W.

To generate the two-photon Fock state for up-conversion, the signal and idler photons from the photon source are first brought to interfere at a telecom-band fiber beam splitter (FBS_C). Next, the output ports 3 and 4 of the FBS_C are connected to two avalanche photon detectors (APD, ID220, free-running (In,Ga)As detector, 20% quantum efficiency, 5-μs dead time, 3-kcps dark counts), from which the output signals are sent to a coincidence device (Timeharp 260, 1.6-ns coincidence window) for coincidence measurement. From the pattern of the HOM interference [Fig. 3(a)] (coincidences between ports 3 and 4), the visibilities are $(97.90 \pm 0.25)\%$ and the two-photon coherent length is 0.83 mm, which corresponds to a bandwidth of 1.28 nm. The high-HOM visibility of the source guarantees that the output ports 3 and 4 of FBS_C are in the maximally entangled state of $1/\sqrt{2}(|20\rangle + |02\rangle)_{1547\ \mathrm{nm}}$. Next, another telecom-band FBS is connected to port 3. The postselection state of this second FBS is $|11\rangle_{1547\ \mathrm{nm}}$, the output of which is connected to the APDs for coincidence measurement; the results are given in Fig. 3(b). When the two photons completely overlap at the first FBS, coincidences between the second FBS are double that when the two photons are completely nonoverlapping. This phenomenon indicates that the output of the first FBS is indeed a two-photon Fock state at the dip of the HOM interference.

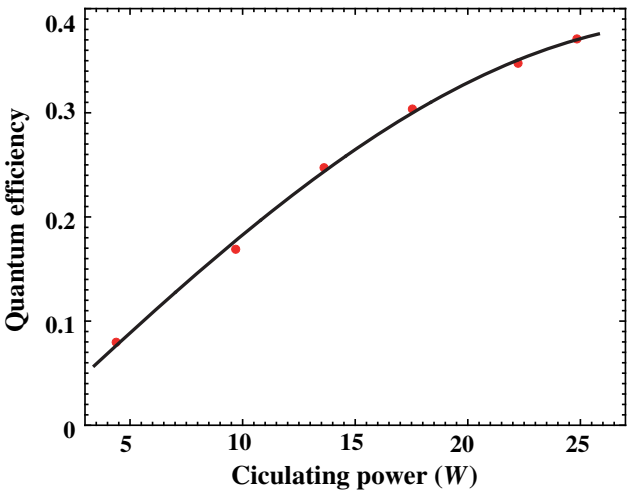

FIG. 2. Internal quantum conversion efficiency as a function of circulation power inside the cavity.

Then the output photon from port 4 is injected into the QFC module [Fig. 1(b)] for frequency up-conversion. The QFC module consists of a 2-cm type-I sum-frequency-generation (SFG) PPKTP crystal inside a ring cavity with a single resonance at 795 nm. The 1547-nm photon is focused into the center of the crystal, and the up-converted 525-nm photon is collected in a single-mode fiber for detection or further processing. The pump powers are fixed at 550 and 520 mW for the two cavities in the experiments to balance the conversion efficiency of the QFCs. The single photon at 1547 nm only single passes the cavity mirrors CM3 and CM4. The ring cavity has two flat mirrors (CM1, CM2) and two concave mirrors (CM3, CM4) with a curvature of 80 mm. The input mirror CM1 has 3% transmittance for 795 nm; CM2 is high reflective coated at 795 nm ($R > 99.9\%$); mirror CM3 is high transmitted coated at 1547 nm ($T > 98\%$) and high reflective coated at 795 nm; mirror CM4 is high reflective coated at 795 nm, high transmitted coated at 1547 nm and 525 nm ($T > 98\%$).

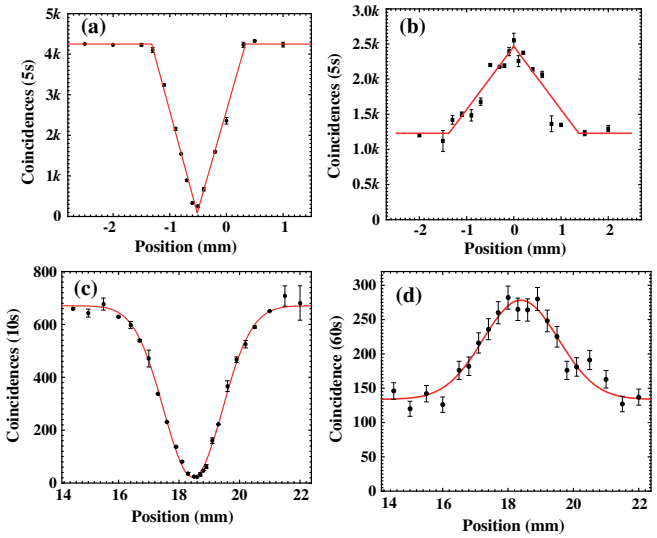

FIG. 3. Experimental results for two-photon Fock state up-conversion. (a) and (c) HOM-interference patterns of the source and after up-conversion. (b) and (d) Coincidence counts after the second FBS for the source and for up-converted photons. Error bars in (d) are evaluated assuming the photon-detection process obeys Poisson statistics.

The beam waists are about 40 μm at the center of the PPKTP crystals. PPKTP crystals have dimensions of 1 mm × 2 mm × 20 mm. The phase-matching temperatures of the two crystals are kept at 51 and 49.5 °C, respectively. The pump beams are modulated with two electro-optical modulators for locking the cavity using the Pound-Drever-Hall method [30].

Two kinds of measurements are performed on the up-converted 525-nm photon. Coincidence counts between the 1547-nm photon (port 3) and the 525-nm photon (port 6) are measured as a function of the position of the air gap [Fig. 3(c)]. Nearly perfect HOM interference is observed with a visibility of $(96.72 \pm 0.82)\%$, and the fitted curve has a Gaussian shape reflecting the filtering effect in the SFG process [31]. For qualitative discussions about the change of the shape of the HOM-interference curve, please refer to Sec. V for details. The SFG bandwidth of the crystal is narrower than the bandwidth of the photon pair (0.5 nm for the 1547-nm photon), which can be seen from the broadening of the bandwidth of the HOM curve. As for the photon source, the up-converted 525-nm photon is split using a 525-nm FBS; the output signals of the FBS are sent to two visible Si APDs (50% quantum efficiency, 300 cps dark count) for coincidence measurements. The results [Fig. 3(d)] show the same behavior as in Fig. 3(b) and demonstrate that the quantum properties of the photon after QFC have been preserved.

IV. QFC OF BOTH PHOTONS AND NOON-STATE INTERFERENCE

Next, both 1547-nm photons are sent to two QFC modules [Fig. 1(d)] for up-converting to 525-nm photons. To demonstrate the indistinguishability of the up-converted 525-nm photons, HOM interference is performed first for the two 525-nm photons where the output signals of the two QFCs are connected to a 525-nm FBS [not shown in Fig. 1(d)]. The interference pattern [Fig. 4(a)] is almost perfect with a visibility of $(97.66 \pm 0.91)\%$, indicating that the up-converted photons are highly indistinguishable. High HOM-interference visibility guarantees that a maximal two-photon NOON state of the form $1/\sqrt{2}(|20\rangle + |02\rangle)_{525\ \mathrm{nm}}$ is generated.

Finally, the up-converted two 525-nm photons are injected into a tilted self-stable Sagnac interferometer for one-photon and two-photon interference measurements [13]. The self-stable interferometer is the key for long-term data acquisition, which is rather different from the traditional Mach-Zehnder interferometer that needs active stabilization if the measurement time is very long. The interferometer contains a phase plate (PP) to vary the phase in one optical path. For one-photon interference, one input port of the interferometer is blocked. A highly attenuated 1547-nm laser beam of single-photon level is used to generate the 525-nm attenuated single photons. The interference fringes obtained as a function of the rotation angle of the phase plate [Fig. 4(b)] give visibility $(97.51 \pm 0.5)\%$. For the two-photon inputs from both input ports of the interferometer, the two-photon interference fringes [Fig. 4(c)] have an oscillation period that is half that of

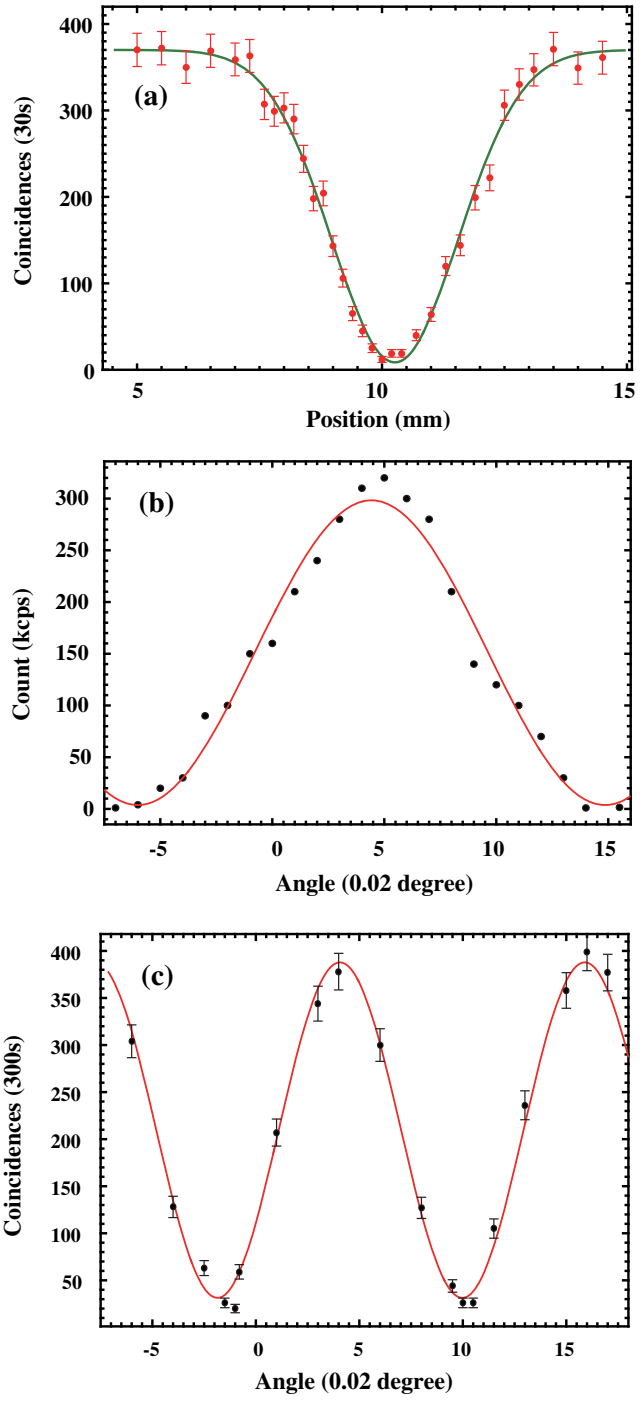

FIG. 4. Experimental results for the generation of 525-nm two-photon NOON states. (a) HOM interference for up-converted 525-nm photon pair. (b) and (c) one-photon and two-photon interference patterns as a function of the rotation angle of the phase plate. Error bars in (a) and (c) are evaluated assuming the photon-detection process obeys Poisson statistics.

the single-photon interference; the visibility of the two-photon interference is $(84.93 \pm 3.18)\%$, which surpasses the SQL threshold (71%) for two-photon NOON states.

Now we will estimate the overall detection efficiency of the photon pairs after being generated from the PPKTP crystal. The average collection efficiency of signal and idler photons of the entangled source is 0.24. In the experiments, the efficiencies include the following: filter transmission (0.80); total transmission of the faces of the crystal, cavity mirror (CM3, CM4), lenses, and wave plates (0.86); the fiber collection efficiencies of the 525-nm SMF (0.60); the bandwidth of the SFG (0.5 nm), which reduced the total quantum efficiency to 0.064; the single-photon-detection efficiency (0.50); the transmission of the air gap (0.8); and the in and out transmission of the self-stable Sagnac-interferometer (0.51). Therefore, the overall detection efficiency of the signal photon is about 2.0×10^{-6}.

V. PHOTON SPECTRA CHANGE IN QFC

For spontaneous parametric down conversion (SPDC) in a type-II PPKTP crystal, the phase mismatching Δk_{II} can be expressed as

$$\Delta k_{\mathrm{II}} = k_p - k_s - k_i + \frac{2\pi}{\Lambda_{\mathrm{II}}}, \tag{4}$$

where $k_j = 2\pi n_j/\lambda_j (j = p, s, i)$ are wave vectors inside the crystal, and Λ_{II} is the periodically poling period of the crystal. For a narrow-bandwidth continuous pump laser beam, the degenerate emission spectra of the crystal can be expressed as

$$F(\lambda_s, \lambda_i, \lambda_p) \propto \mathrm{sinc}^2\left(\frac{\Delta k_{\mathrm{II}} L_{\mathrm{II}}}{2}\right), \tag{5}$$

where L_{II} is the crystal length. By inserting the Sellmeier equation for n_y and n_z into Eq. (5) [32,33], we can obtain the emission spectra for the generated photon pairs. The numerical simulation results are given in Fig. 5(a), the bandwidth of the numerical calculation is about 1.3 nm. Because the spectra of the signal and idler photon are the sinc^2 function, therefore, the HOM-interference pattern should be a reversed triangle, as the HOM-interference shape is the Fourier transformation of the joint spectra of the signal and idler; one can refer to Ref. [31] for details.

The SFG crystal used in our experiments is a type-I quasi-phase-matching PPKTP crystal, the phase mismatching can be expressed as

$$\Delta k_{\mathrm{I}} = k_{\mathrm{SFG}} - k_p - k_s + \frac{2\pi}{\Lambda_{\mathrm{I}}}, \tag{6}$$

where $k_j = 2\pi n_j/\lambda_j (j = \mathrm{SFG}, p, s)$ are wave vectors inside the crystal. Λ_{I} is the periodically poling period of

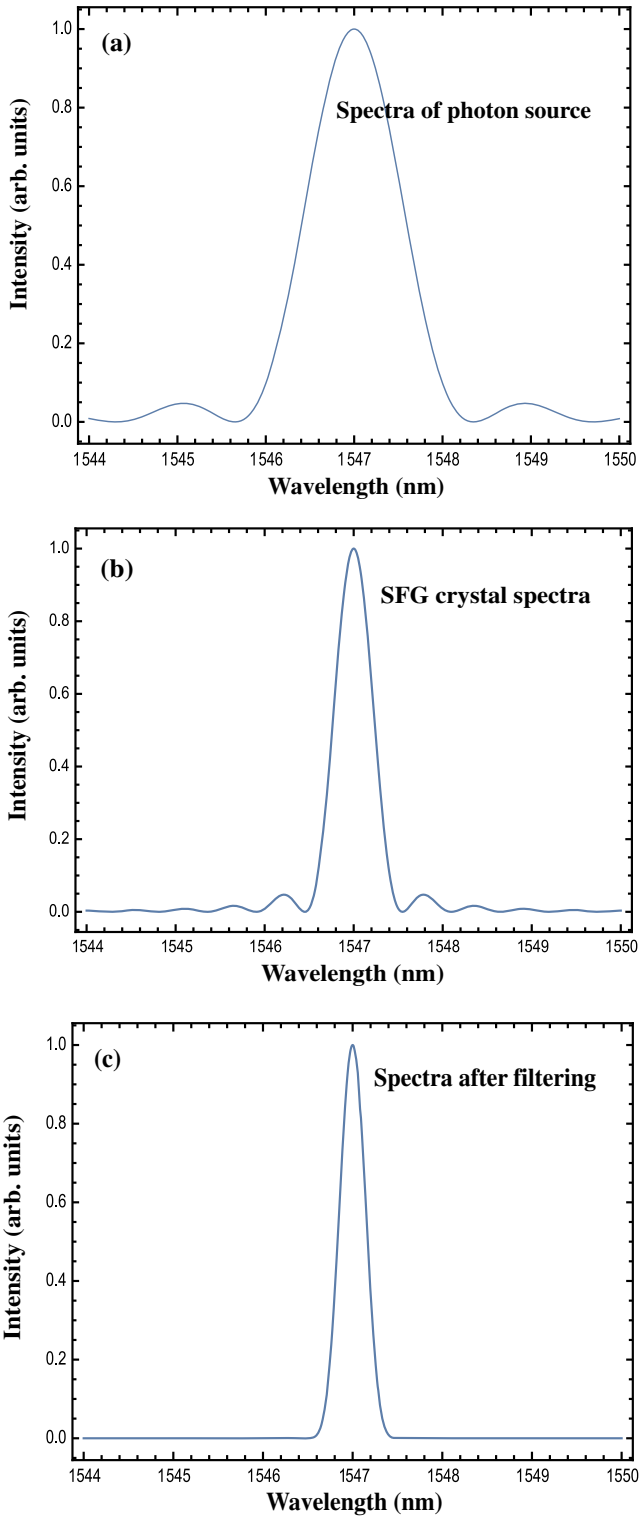

FIG. 5. (a) The emission spectra of the signal and idler photon generated from type-II PPKTP crystal based on SPDC. (b) The acceptance spectra for the SFG crystal. (c) The filtered spectra for the photon pair after being up-converted.

the crystal. For a narrow-bandwidth continuous pump laser beam, the acceptance spectra of the signal photon can be expressed as

$$G(\lambda_s, \lambda_i, \lambda_p) \propto \mathrm{sinc}^2\left(\frac{\Delta k_\mathrm{I} L_\mathrm{I}}{2}\right), \quad (7)$$

where L_I is the crystal length. By inserting the Sellmeier equation of n_z into Eq. (5) [33], we can obtain the acceptance spectra of the signal photon. The numerical simulation results are given in Fig. 5(b), the bandwidth of the numerical calculation is about 0.5 nm.

The SFG process can be viewed as a spectra filtering process for the signal and idler photon, therefore effective spectra for the photon pairs after SFG can be expressed as

$$\begin{aligned}\Gamma(\lambda_s, \lambda_i, \lambda_p) &\propto F(\lambda_s, \lambda_i, \lambda_p) G(\lambda_s, \lambda_i, \lambda_p)^2 \\ &= \mathrm{sinc}^2\left(\frac{\Delta k_\mathrm{II} L_\mathrm{II}}{2}\right) \mathrm{sinc}^4\left(\frac{\Delta k_\mathrm{I} L_\mathrm{I}}{2}\right). \quad (8)\end{aligned}$$

The simulation of the spectra of the up-converted photon pair is shown in Fig. 5(c). After being up-converted, the spectra of the photon pair will change from the sinc^2 function to the quasi-Gaussian function, and it will be well approximated by using Gaussian function. This is the reason to use the Gaussian function to fit the HOM-interference data for the up-converted photon pair.

VI. CONLUSIONS AND OUTLOOK

In summary, QFC for the two-photon Fock state and both photons in the pair are realized in this work. We also verify the interference of the generated two-photon NOON state. The change of the photon spectra in the up-conversion process is investigated in detail. Our results demonstrate that the single-photon properties and the indistinguishability are preserved during frequency conversion. Using QFC, we demonstrate a promising technique to generate a short-wavelength multi-photon NOON state that has a similar effect in increasing the photon number at the fundamental photon wavelength. The de Broglie wavelength of the 525-nm two-photon NOON state thus generated is equivalent to a six-photon NOON state at 1547 nm. The 525-nm two-photon interference has a visibility high enough to surpass the SQL.

The remaining problem to be solved for practical applications of the presented technique is the quantum conversion efficiency. If this efficiency reaches unity, higher-photon-number NOON states at longer wavelengths can be directly converted to short-wavelength NOON states. The efficiency of the conversion can be solved using longer SFG crystals and a better cavity mirror coating with lower cavity losses. We want to point out that by changing the crystal parameters and the pump wavelength, the up-converted photon wavelength can be extended to the UV regime, which can be shorter than the 390-nm photon pairs reported in Ref. [25]. Once the phase plate used in the experiment is replaced by transparent optical materials, we can determine their optical properties such as dispersion, absorption, and surface imaging with high precision, which may beat the SQL. The spectra filtering effect in this work can be used for constructing all optical bandpass and notch filters for the single photon, which will be useful in engineering the spectra of the photon source. This work paves the way for QFC of high-number multiparticle entangled states, offering the prospect of alternative techniques for high-precision quantum metrology.

ACKNOWLEDGMENTS

This work is supported by the National Natural Science Foundation of China (Grants No. 11604322, No. 61275115, No. 61435011, No. 61525504, and No. 61605194), the China Postdoctoral Science Foundation (Grant No. 2016M590570), and the Fundamental Research Funds for the Central Universities.

Z.-Y. Z. and S.-L. L. contributed equally to this work.

[1] V. Giovannetti, S. Lloyd, and L. Maccone, Quantum-enhanced measurements: Beating the standard quantum limit, Science **306**, 1330 (2004).
[2] T. Roger, S. Restuccia, A. Lyons, D. Giovannini, J. Romero, J. Jeffers, M. Padgett, and D. Faccio, Coherent Absorption of NOON States, Phys. Rev. Lett. **117**, 023601 (2016).
[3] T. Ono, R. Okamoto, and S. Takeuchi, An entanglement-enhanced microscope, Nat. Commun. **4**, 2426 (2013).
[4] J. A. Jones, S. D. Karlen, J. Fitzsimons, A. Ardavan, S. C. Benjamin, G. A. D. Briggs, and J. J. L. Morton, Magnetic field sensing beyond the standard quantum limit using 10-spin NOON states, Science **324**, 1166 (2009).
[5] J. Jacobson, G. Bjork, I. Chuang, and Y. Yamamoto, Photonic de Broglie Waves, Phys. Rev. Lett. **74**, 4835 (1995).
[6] J. G. Rarity, P. R. Tapster, E. Jakeman, T. Larchuk, R. A. Campos, M. C. Teich, and B. E. A. Saleh, Two-Photon Interference in a Mach-Zehnder Interferometer, Phys. Rev. Lett. **65**, 1348 (1990).
[7] K. Edamatsu, R. Shimizu, and T. Itoh, Measurement of the Photonic de Broglie Wavelength of Entangled Photon Pairs Generated by Spontaneous Parametric Down-Conversion, Phys. Rev. Lett. **89**, 213601 (2002).
[8] M. W. Mitchell, J. S. Lundeen, and A. M. Steinberg, Super-resolving phase measurements with a multiphoton entangled state, Nature (London) **429**, 161 (2004).
[9] P. Walther, J.-W. Pan, M. Aspelmeyer, R. Ursin, S. Gasparoni, and A. Zeilinger, De Broglie wavelength of a non-local four-photon state, Nature (London) **429**, 158 (2004).
[10] H. S. Eisenberg, J. F. Hodelin, G. Khoury, and D. Bouwmeester, Multiphoton Path Entanglement by Nonlocal Bunching, Phys. Rev. Lett. **94**, 090502 (2005).
[11] K. J. Resch, K. L. Pregnell, R. Prevedel, A. Gilchrist, G. J. Pryde, J. L. O'Brien, and A. G. White, Time-Reversal and Super-Resolving Phase Measurements, Phys. Rev. Lett. **98**, 223601 (2007).

[12] I. Afek, O. Ambar, and Y. Silberberg, High-NOON states by mixing quantum and classical light, Science **328**, 879 (2010).

[13] T. Nagata, R. Okamoto, J. L. O'Brien, K. Sasaki, and S. Takeuchi, Beating the standard quantum limit with four-entangled photons, Science **316**, 726 (2007).

[14] Y. Kawabe, H. Fujiwara, R. Okamoto, K. Sasaki, and S. Takeuchi, Quantum interference fringes beating the diffraction limit, Opt. Express **15**, 14244 (2007).

[15] Y.-S. Kim, O. Kwon, S. M. Lee, J.-C. Lee, H. Kim, S.-K. Choi, H. Su Park, and Y.-H. Kim, Observation of Young's double-slit interference with the three-photon NOON state, Opt. Express **19**, 24957 (2011).

[16] P. Kumar, Quantum frequency conversion, Opt. Lett. **15**, 1476 (1990).

[17] Y.-H. Kim, S. P. Kulik, and Y. Shih, Quantum Teleportation of a Polarization State with a Complete Bell State Measurement, Phys. Rev. Lett. **86**, 1370 (2001).

[18] S. Tanzilli, W. Tittel, M. Halder, O. Alibart, P. Baldi, N. Gisin, and H. Zbinden, A photonic quantum information interface, Nature (London) **437**, 116 (2005).

[19] M. T. Rakher, L. Ma, O. Slattery, X. Tang, and K. Srinivasan, Quantum transduction of telecommunications-band single photons from a quantum dot by frequency upconversion, Nat. Photonics **4**, 786 (2010).

[20] C. E. Vollmer, C. Baune, A. Samblowski, T. Eberle, V. Hndchen, J. Fiurek, and R. Schnabel, Quantum Up-Conversion of Squeezed Vacuum States from 1550 to 532 nm, Phys. Rev. Lett. **112**, 073602 (2014).

[21] Z.-Y. Zhou, Y. Li, D.-S. Ding, W. Zhang, S. Shi, B.-S. Shi, and G.-C. Guo, Orbital angular momentum photonic quantum interface, Light Sci. Appl. **5**, e16019 (2016).

[22] Z.-Y. Zhou, S.-L. Liu, Y. Li, D.-S. Ding, W. Zhang, S. Shi, M.-X. Dong, B.-S. Shi, and G.-C. Guo, Orbital Angular Momentum-Entanglement Frequency Transducer, Phys. Rev. Lett. **117**, 103601 (2016).

[23] G.-L. Shentu, J. S. Pelc, X.-D. Wang, Q.-C. Sun, M.-Y. Zheng, M. M. Fejer, Q. Zhang, and J.-W. Pan, Ultralow noise up-conversion detector and spectrometer for the telecom band, Opt. Express **21**, 13986 (2013).

[24] T. Kobayashi, R. Ikuta, S. Yasui, S. Miki, T. Yamashita, H. Terai, T. Yamamoto, M. Koashi, and N. Imoto, Frequency-domain Hong-Ou-Mandel interference, Nat. Photonics **10**, 441 (2016).

[25] K. Edamatsu, G. Oohata, R. Shimizu, and T. Itoh, Generation of ultraviolet entangled photons in a semiconductor, Nature (London) **431**, 167 (2004).

[26] H. Takesue, Erasing Distinguishability Using Quantum Frequency Up-Conversion, Phys. Rev. Lett. **101**, 173901 (2008).

[27] S. Gerber, D. Rotter, M. Hennrich, R. Blatt, F. Rohde, C. Schuck, M. Almendros, R. Gehr, F. Dubin, and J. Eschner, Quantum interference from remotely trapped ions, New J. Phys. **11**, 013032 (2009).

[28] Y. Li, Z.-Y. Zhou, D.-S. Ding, and B.-S. Shi, CW-pumped telecom band polarization entangled photon pair generation in a Sagnac interferometer, Opt. Express **23**, 28792 (2015).

[29] Z.-H. Han, S.-L. Liu, S.-K. Liu, D.-S. Ding, and Z.-Y. Zhou, Efficient frequency doubling at 776 nm in a ring cavity, Opt. Commun. **396**, 146 (2017).

[30] R. W. P. Drever, J. L. Hall, F. V. Kowalski, J. Hough, G. M. Ford, A. J. Munley, and H. Ward, Laser phase and frequency stabilization using and optical resonator, Appl. Phys. B **31**, 97 (1983).

[31] M. H. Rubin, D. N. Klyshko, Y. H. Shih, and A. V. Sergienko, Theory of two-photon entanglement in type-II optical parametric down-conversion, Phys. Rev. A **50**, 5122 (1994).

[32] F. Konig and F. N. C. Wong, Extended phase matching of second-harmonic generation in periodically poled KTiOPO4 with zero group-velocity mismatch, Appl. Phys. Lett. **84**, 1644 (2004).

[33] K. Fradkin, A. Arie, A. Skliar, and G. Rosenman, Tunable midinfrared source by difference frequency generation in bulk periodically poled $KTiOPO_4$, Appl. Phys. Lett. **74**, 914 (1999).